*Publication costs of this article were assisted by Texas Instruments Incorporated.*

REFERENCES

1. W. Kaiser, H. L. Frisch, and H. Reiss, *Phys. Rev.*, **112**, 1546 (1958).
2. C. S. Fuller, F. H. Doleiden, and K. Wolfstirn, *J. Phys. Chem. Solids*, **13**, 187 (1960).
3. J. A. Baker, *Solid-State Electron.*, **13**, 1431 (1970).
4. Y. Takano and M. Maki, "Semiconductor Silicon 1973," H. R. Huff and R. R. Burgess, Editors, The Electrochemical Society Softbound Symposium Series, Princeton, N.J. (1973).

# Properties of Liquid Phase Epitaxial $In_{1-x}Ga_xAs$ ($x \cong 0.5$) on InP Substrate

**Yoshikazu Takeda, Akio Sasaki, Yujiro Imamura, and Toshinori Takagi**

*Department of Electronics, Kyoto University, Kyoto, Japan*

ABSTRACT

Undoped $In_{1-x}Ga_xAs$ ($x \cong 0.5$) crystal films with very homogeneous composition were grown on InP substrates by liquid phase epitaxy. Study was made on physical, electrical, and optical properties of this mixed crystal. The growth temperature was varied between 550° and 750°C. All the crystals were n-type. The electron mobility was found to vary from 5240 to 8500 $cm^2\ V^{-1}\ sec^{-1}$ and the electron concentration from $6.3 \times 10^{16}$ to $1.3 \times 10^{16}\ cm^{-3}$ at 300°K. Etch pit density and half-width of photoluminescence spectra decreased with increasing growth temperature. High quality crystals were grown at around 700°C.

Much interest has been recently focused on $In_{1-x}Ga_xAs$ mixed crystal because of its applications to optical sources (1-3) and detectors (4) in the 1.06 $\mu$m low loss region of optical fibers (5). Efficient light-emitting diodes and room temperature laser diodes were fabricated with this material. Another potential application of this mixed crystal is for high frequency devices (6).

The mixed crystal can be designed to have larger bandgaps than InAs and higher mobilities than GaAs. Near middle composition the bandgap, $E_g$, is about 0.75 eV at which the extrinsic carrier concentration ($>10^{15}\ cm^{-3}$) is not affected by the temperature variations of the intrinsic carrier concentration ($\sim 10^{11}\ cm^{-3}$) around room temperature. Further, the energy separation, $\Delta E$, between the central and the satellite valleys in the conduction band becomes wider with the increase of the InAs mole fraction. Near $x \cong 0.5$, $E_g$ is expected to equal $\Delta E$. This does not make the electron velocity decreased by the transferred electron effect. Thus, $In_{1-x}Ga_xAs$ ($x \cong 0.5$) can be considered better suited for high frequency field-effect transistors and high speed switching devices than GaAs or InP (6).

The $In_{1-x}Ga_xAs$ epitaxial films of around middle composition ($x \cong 0.5$) have been grown by vapor phase epitaxy on GaAs (7-8) and $Al_2O_3$ (9) substrates. Fairly high electron mobilities and the electron scattering analysis were reported by Glicksman *et al.* (10) for $In_{1-x}Ga_xAs$ ($0.75 \leqq x \leqq 1$). However, the mobilities around 6000 $cm^2\ V^{-1}\ sec^{-1}$ are not higher than those of GaAs. Bulk $In_{1-x}Ga_xAs$ crystals have shown very high mobilities (11-12) as compared with epitaxial mixed crystals of around middle composition, but it is difficult to grow single crystals uniform in composition. The difficulty is attributed to large difference between the liquidus and solidus. Single crystals with nonuniform composition are not suitable for most device applications.

A uniform and good crystalline $In_{1-x}Ga_xAs$ can be grown on GaAs by using stepwise (2) or continuous (14-15) compositional grading to take up the lattice mismatch between the substrate and the desired composition layers. However, with the grading process it is not easy to reach $In_{1-x}Ga_xAs$ ($x \cong 0.5$) from GaAs substrate nor is it suitable for mass production. The lattice constant of InP lies in the middle of the lattice constants of InAs and GaAs, matching with that of $In_{0.53}Ga_{0.47}As$, when Vegard's law is applied to $In_{1-x}Ga_xAs$. Moreover, semi-insulating InP substrates, although not yet developed enough, are available which facilitate electrical evaluation of the grown layers and device applications. It has been reported by Sasaki *et al.* (16) that $In_{1-x}Ga_xAs$ ($x \cong 0.5$) can be grown directly on InP by liquid phase epitaxy. Recently, the conditions for LPE growth of $In_{0.53}Ga_{0.47}As$ have been discussed by Sankaran *et al.* (17). Electron mobility and energy gap of LPE $In_{0.53}Ga_{0.47}As$ on InP have been reported by Takeda *et al.* (18).

In this paper, we describe a study on the properties of $In_{1-x}Ga_xAs$ ($x \cong 0.5$) grown on InP from a melt with a theoretical solidus composition of $x = 0.5$ at each growth temperature. Single crystals of $x \cong 0.5$ are grown on semi-insulating InP substrates by liquid phase epitaxy. The growth temperature (the initial temperature at which the melt is brought over the substrate is called the growth temperature in this paper, since the temperature is lowered in this growth process) is varied from 500° to 800°C keeping the other conditions, such as the melt-baking temperature and interval, the cooling rate and interval, and the substrate orientation, the same. Thickness, surface morphology, etch pit density, composition, photoluminescence, electron mobility, and electron concentration of the grown layers are examined.

## Experimental Procedures

*Crystal growth.*—Liquid phase epitaxial growth is carried out in a horizontal graphite boat and slider assembly in a Pd-diffused flowing hydrogen ambient. All the mixed crystals are grown on the Cr-doped ($\rho > 10^3\ \Omega$cm), (111)B-oriented InP substrates. Growth temperatures are chosen at 50°C intervals from 500° to 800°C. The cooling rate is 0.15°C/min, and the cooling interval is about 10°C at each growth temperature.

Starting materials are six 9's pure In, seven 9's pure Ga (Mitsubishi Metal Mining Company, Limited),

Key words: InGaAs, LPE, heteroepitaxy, InP substrate.

and undoped polycrystalline InAs ($n = 1 \sim 3 \times 10^{16}$ $cm^{-3}$ and $\mu = 20{,}000 \sim 23{,}000$ $cm^2$ $V^{-1}$ $sec^{-1}$) (Sumitomo Electric Industries, Limited). The Ga is not etched, but the In is etched with a 5% HCl:$H_2O_2$ solution, and the InAs with a 1% Br:methanol solution just prior to loading. Polished InP substrates are etched with a 1% Br:methanol solution for 2 min. The melts are about 2g, and a slight excess of InAs is added to ensure As saturation in the melt. The substrate dimensions are $10 \times 5 \times 0.4$ $mm^3$.

Prior to growth, In and Ga are baked in a flowing hydrogen ambient at 800°C for 3 hr to mix the In atoms and Ga atoms. In order to minimize the thermal etching of the substrate surface and to avoid the deviation of the melt composition due to the loss of As during the baking treatment at a high temperature, the substrate and the InAs are introduced to the furnace after cooling the melt to room temperature. The substrate is placed in a recess of the boat and is covered with the slider to minimize thermal etching during the saturation time of the melt.

The phase diagram was calculated according to Wu and Pearson's model (19), and the ternary melt having a solidus composition of $In_{0.50}Ga_{0.50}As$ is used at each growth temperature. The melt compositions are given in Table I.

*Composition.*—The composition is determined by x-ray diffraction of the Cu-$K_{\alpha 1}$ radiation using Vegard's law which can be applied to this mixed crystal (20). At high diffraction angles such as for (333) or (444) reflections, both reflections from the epitaxial layer and the substrate are detected. Since the diffraction angle of the InP substrate is known, the precise diffraction angle of the mixed crystal is determined from (333) or (444) reflection using the substrate reflection as an internal standard.

*Photoluminescence (PL).*—The photoluminescence excited by a He-Ne laser (6328Å) is detected by a PbS photoconductive diode cooled with a Dry Ice:ethanol solution. A conventional lock-in technique is used. The spectral response of the total system is in the range from 1.4 to 2.3 $\mu$m (at half-responses). After being lightly etched with a 1% Br:methanol solution, the sample is attached to a copper jig and immersed in liquid nitrogen contained in a double wall Dewar. All the samples are angle-lapped at 3° to examine the spectral variations along the thickness of the grown layers. The sample is moved parallel to the angle-lapped surface by a manipulator to which the copper jig is attached.

*Resistivity and Hall coefficient measurement.*—The method of van der Pauw (21) is used to determine the resistivity and the Hall coefficient. Typical sample dimensions for the measurements are $4 \times 4$ $mm^2$ and the thickness of the epitaxial layers varied from 3 to 24 $\mu$m. Pure indium dots (usually about 300 $\mu$m in diameter) are alloyed for contact electrodes at the corners of the grown layers in a flowing hydrogen ambient at 450°C for 1 min. Prior to the alloying, the surface is lightly etched with a 1% Br:methanol solution.

The sample temperature is varied from 77°K (immersed in liquid nitrogen) to 300°K and controlled to be stable within ±0.5°K. The source current is 20 or 100 $\mu$A, and the magnetic field for the Hall coefficient measurement is 5 kG.

**Table I. Calculated weight of Ga and InAs per gram of In of melt for solidus $In_{0.50}Ga_{0.50}As$**

| $T_G$ (°C) | In (g) | Ga (mg) | InAs (mg) |
|---|---|---|---|
| 500 | 1.000 | 10.27 | 13.80 |
| 550 | 1.000 | 13.84 | 29.94 |
| 600 | 1.000 | 18.08 | 58.55 |
| 650 | 1.000 | 23.14 | 104.67 |
| 700 | 1.000 | 29.27 | 174.12 |
| 750 | 1.000 | 36.82 | 275.32 |
| 800 | 1.000 | 46.58 | 423.96 |

## Results and Discussion

*Thermal etching of InP substrate surface.*—Examples of the substrate (111)B-surface baked at 500° and 750°C for 1 hr in a flowing hydrogen ambient are shown in Fig. 1, (a) and (b), respectively. The substrates are placed in a recess of the boat and covered with the slider during the heat-treatment. The substrate surface shows evidence of thermal etching. Small droplets remain on the surface at a lower temperature, and larger droplets at a higher temperature. A large droplet is seen to be due the coalescence of small droplets. The droplets are identified to be In by the electron probe microanalyzer (EPMA), and this thermal etching is due to the thermal decomposition of InP at a high temperature. Similar observations have been reported by Pak *et al.* (22). This etching effect influences the thickness and the surface morphology of the grown layer as is shown next.

*Thickness and surface morphology.*—As-grown surfaces and cleaved cross sections of the epitaxial layers grown at 500° and 700°C are shown in Fig. 2 (a) and (b), respectively. The as-grown surface at 700°C is the smoothest among those grown in the range from 500° to 800°C. At temperatures below 650°C, the surface becomes rough. Melt droplets are left on the as-grown surface during wiping due to the surface roughness. The thickness of epitaxial layer decreases exponentially with decreasing growth temperature. At 500°C no layer is grown, and this can be attributed to the low solubility of As at 500°C. At temperatures above 750°C, the as-grown surface is also rough. This is confirmed to be caused by the roughness of the substrate surface as a result of the thermal etching. At 800°C the melt remains almost over the entire surface after wiping. However, a uniform layer would be grown if the problem of the thermal etching is overcome by keeping the phosphorus over-pressure

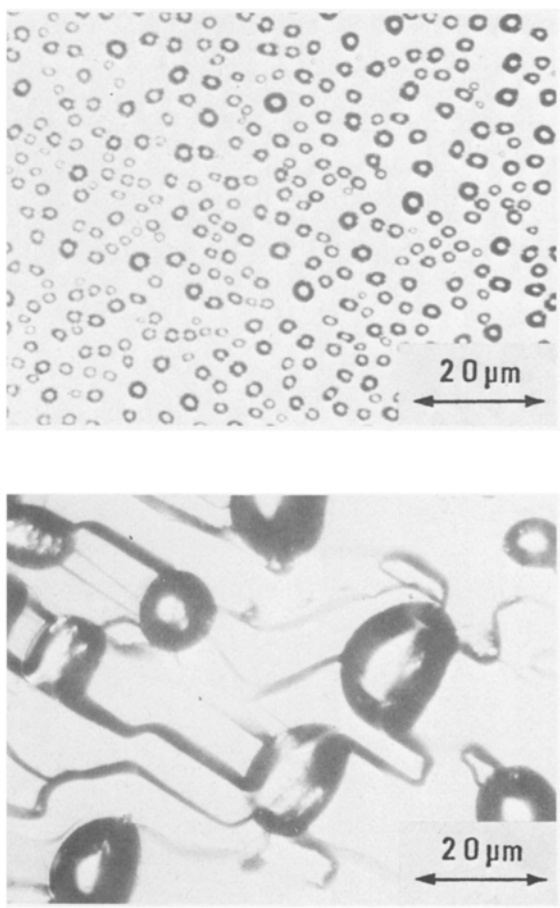


**Fig. 1. Examples of the thermal etching of InP substrate surface after 1 hr baking at 550°C (a, top) and 750°C (b, bottom) in a flowing hydrogen ambient.**

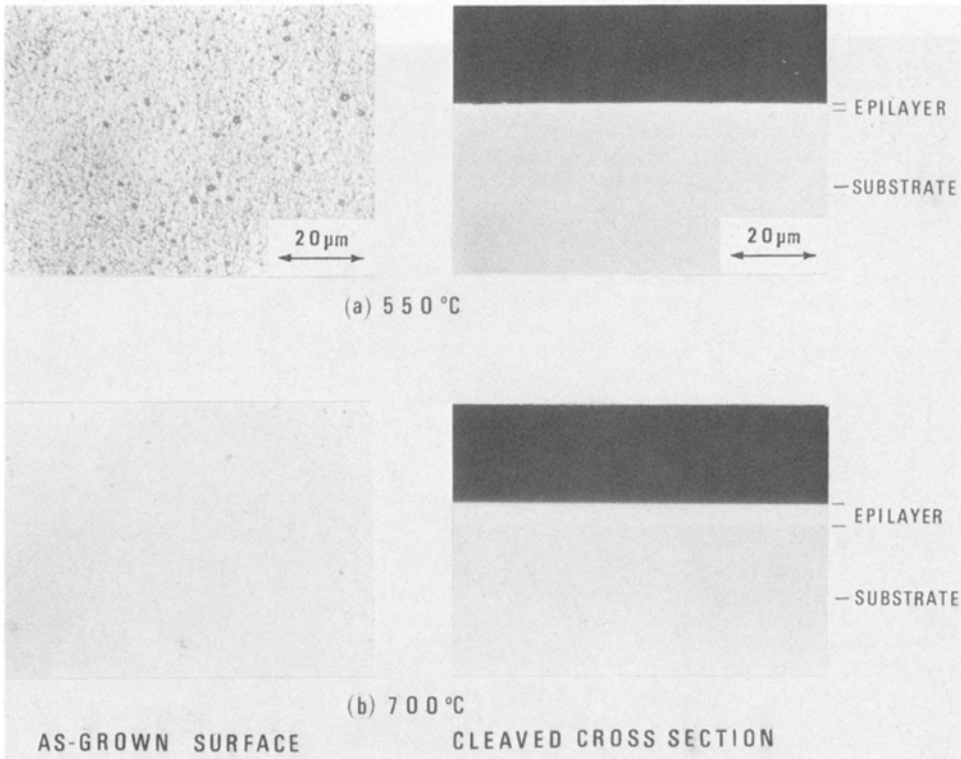


**Fig. 2. As-grown surfaces and as-cleaved cross sections of the epitaxial layers grown at 550°C (a) and 700°C (b). Small spots are droplets of melts remaining on rough surface. No inclusions are found in cleaved sections.**

or by etching back the InP surface. In the experiments all the mixed crystals grown at 800°C are excluded from the measurements.

In Fig. 3 the temperature dependence of the layer thickness normalized with the In weight in the melt ($W_{In}$) and the cooling interval ($T_c$) is shown. Between 550° and 700°C, the curve follows qualitatively the temperature dependence of the As fraction in the melt. The abrupt decrease at 750°C could be explained as follows. A fair amount of In remains on the substrate surface due to the thermal etching, as shown in Fig. 2. The melt when contacted with the substrate is diluted by this In and undersaturated at the interface. Therefore, the initial cooling period is spent in re-equilibration and resaturation and the layer thickness is small. No In inclusions are found at the interface of the layers, indicating that all the In droplets are taken into the contacted melt before the growth begins.

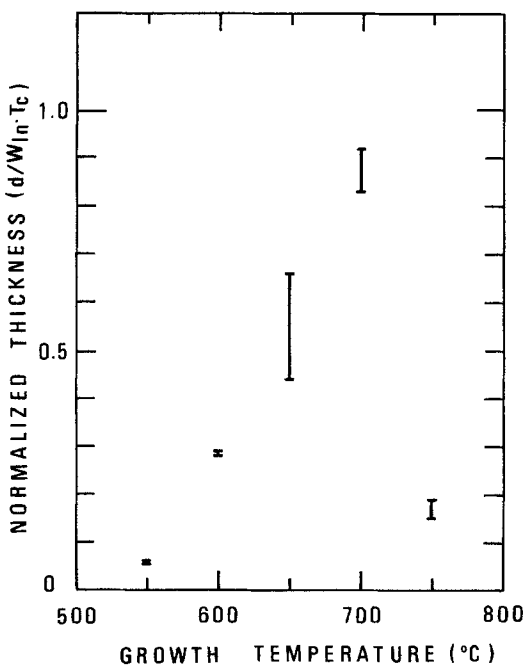


**Fig. 3. Layer thickness as a function of growth temperature. The thickness is normalized to In weight ($W_{In}$) and cooling interval ($T_c$). The bar length corresponds to variation from sample to sample.**

*Etch pit density (EPD).*—Etch pits in the grown layers are revealed by etching with an A-B solution (23) for 10-30 sec at room temperature. The average density at each growth temperature is listed in Table II. In the sample grown at 550°C the EPD is too high to count, far beyond $10^6$ cm$^{-2}$. This high EPD may be in part due to the relatively large lattice mismatch between the substrate and the layer as is shown in Fig. 4. Better crystals could be grown even at temperatures below 650°C by precisely matching the lattice constant. About $1 \times 10^5$ cm$^{-2}$ may be the lower limit of the EPD, because the Cr-doped InP substrate has approximately the same density of etch pits as revealed by etching with an R-C solution (24) for 10 min at 60°C.

*Composition.*—The composition *vs.* growth temperature is shown in Fig. 4. Although the In-Ga-As solution with the solidus composition of $In_{0.50}Ga_{0.50}As$ at each growth temperature is used, the composition of the mixed crystals grown at temperatures between 650° and 750°C is $In_{0.53}Ga_{0.47}As$ at which the lattice constant of the grown layer matches with that of InP. Below 650°C, the mismatch becomes greater with decreasing temperature.

As pointed out by Wu and Pearson (19) the accuracy of the solidus data in their experiment is ±3 mole percent. In our experiments at 600° and 550°C the deviation is over this range. It is possible that the lower Ga composition obtained at these temperatures is due to the inaccuracy of the Wu and Pearson phase diagram. Only a few experimental

**Table II. Average EPD of mixed crystals at each growth temperature**

| Growth temperature (°C) | Average EPD (cm$^{-2}$) |
|---|---|
| 550 | $>>1 \times 10^6$ |
| 600 | $>1 \times 10^6$ |
| 650 | $>5 \times 10^5$ |
| 700 | $\sim 5 \times 10^5$ |
| 750 | $\sim 1 \times 10^6$ |

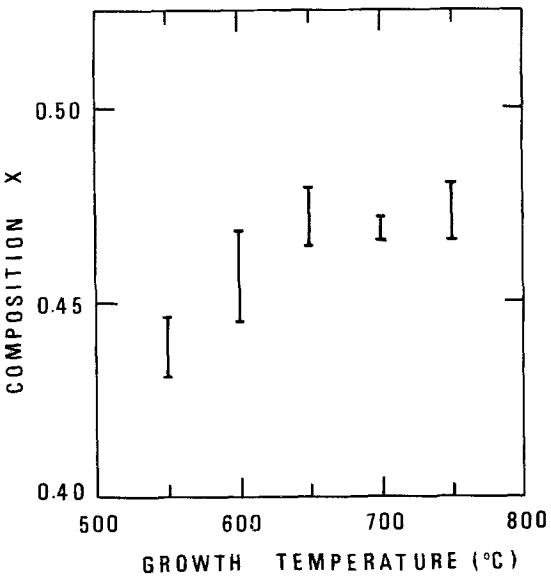


**Fig. 4. Composition *vs.* growth temperature. The In-Ga-As solution of solidus composition $x = 0.5$ is used at each growth temperature.**

data were examined in their phase diagram calculation at these lower temperatures.

Between 650° and 750°C the compositions of the grown layers are within the accuracy of the phase diagram and almost lattice-matched ($x \sim 0.47$) to the InP substrate. It could be considered that at these temperatures lattice-matched layers are obtained at the lower limit 0.47 (=0.50-0.03) of the accuracy of the phase diagram, but there may be another possibility that the lattice-matched layer is forcibly grown by the composition latching in the growth of InGaAs on InP in a certain range of composition as was observed by Stringfellow (25) in the LPE growth of InGaP on GaAs. Further investigations are being carried out on these phenomena and on the determination of the optimum melt composition for lattice matching at each growth temperature.

Continuous layers are obtained from melts of slightly deviated composition from 0.50, but from melts of 0.40 and 0.70 at 700°C only island growth, shown in Fig. 5, is observed as reported by Sankaran *et al.* (17).

An example of the (444) reflections is shown in Fig. 6. The reflections from the epitaxial layer and the substrate are detected at this high angle, and from these peaks a mismatch of $6.6 \times 10^{-4}$ is calculated. The $K_{\alpha 1}$ and $K_{\alpha 2}$ peaks are clearly resolved, indicating good homogeneity of this mixed crystal which is grown at 750°C. The half-width of the peak from the epitaxial layer increases with decreasing growth temperature.

*Photoluminescence.*—Emission spectra of two epitaxial layer surfaces grown at different temperatures

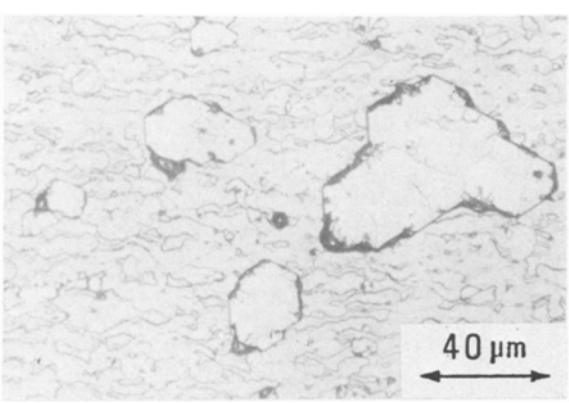


**Fig. 5. Island growth of InGaAs on InP substrate grown at 700°C from the melt of a solidus composition $x = 0.4$.**

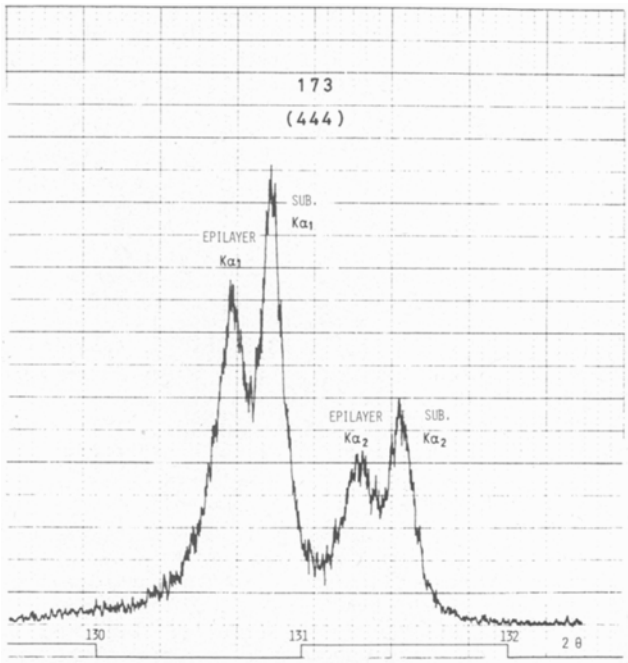


**Fig. 6. An example of (444) x-ray reflections from the $In_{1-x}Ga_xAs$ layer and the InP substrate. $K_{\alpha 1}$ and $K_{\alpha 2}$ peaks from both crystals are clearly resolved.**

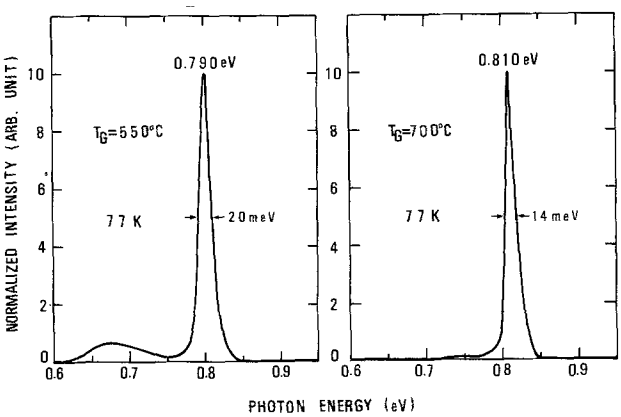


**Fig. 7. Photoluminescence spectra (77°K) of two epitaxial layers grown at 550°C (a) and 700°C (b).**

are compared in Fig. 7. There are two distinctions in the spectra: the photon energy at peak intensity and the half-width. The compositions determined by the photon energies at peak intensities are close to those in Fig. 4 obtained by x-ray diffraction. A good fit to the photon energy ($h\nu$) *vs.* composition ($x$), in the region $0.43 < x < 0.48$ and at $x = 0$, InAs, and $x = 1$, GaAs, at 77°K is given by

$$h\nu(\text{eV}) = 0.404 + 0.649x + 0.457x^2$$

The curve gives quite the same values as those by Wu and Pearson at 77°K (19).

The full width at half-maximum (FWHM) of the spectra decreases linearly with the increase of the growth temperature, *i.e.*, from ~20 meV at 550°C to ~14 meV at 750°C. This dependence is not based on the composition variation across the grown layer within the penetration depth of the He-Ne laser beam. Such a composition variation can be expected from the phase diagram (19); however, the lower the growth temperature, the smaller the composition variation for a cooling interval of 10°C at $x \cong 0.5$. Furthermore, in the experiments, the composition variation from near the interface to the surface is measured to be within ±1% by the EPMA and the photoluminescence. Moreover, the penetration depth of the

laser beam is less than 1 $\mu$m. Along with the growth temperature dependence of the half-width of x-ray reflection peak, it is understood that mixed crystals of better composition homogeneity are grown at higher temperature.

The variation of the photon energy at peak intensity, the intensity, and the FWHM along the angle-lapped grown layer are shown in Fig. 8 for sample 153 as an example. Constant photon energy indicates the uniformity in the composition, and very small variations of the intensity and the FWHM show a homogeneous crystal quality across the grown layer. Similar results are obtained in every sample at different growth temperatures. A relatively low intensity near the interface is due to the finite diameter of the laser beam (~50 $\mu$m), *i.e.*, at distance 0 $\mu$m, most of the laser spot irradiates the substrate and at about 3 $\mu$m (corresponding to about 50 $\mu$m in a layer angle-lapped by 3°) the whole spot is on the grown layer.

*Electrical properties.*—The highest electron mobilities at different growth temperatures are listed in Table III along with electron concentrations and compositions. In the table, the data of GaAs grown in the same growth system at 800°C are shown for comparison. All the grown mixed crystals are n-type with excess carrier concentrations of the order of $10^{16}$ cm$^{-3}$. Our experiments indicate the general tendency that the mobility increases while the concentration decreases with increasing growth temperature. An observation similar to this has been made in the case of InP grown at temperatures between 540° and 780°C by LPE on InP (26). It seems from Table III that better mixed crystals (with higher mobility and lower concentration) can be grown at higher temperatures. But the epitaxial layer is nonuniform at high temperatures due to the thermal etching of the substrate surface. Invariably, the mobility of the mixed crystals increases with decreasing lattice temperature in contrast to Conrad's (7) and Baliga's (8) data. Both 8500 cm$^2$ V$^{-1}$ sec$^{-1}$ at 300°K and 22,100 cm$^2$ V$^{-1}$ sec$^{-1}$ at 77°K of sample 173 are significantly high in the epitaxial $In_{1-x}Ga_xAs$ ($x \cong 0.5$) (7-8, 14) and comparable to those of bulk grown mixed crystals (11-13).

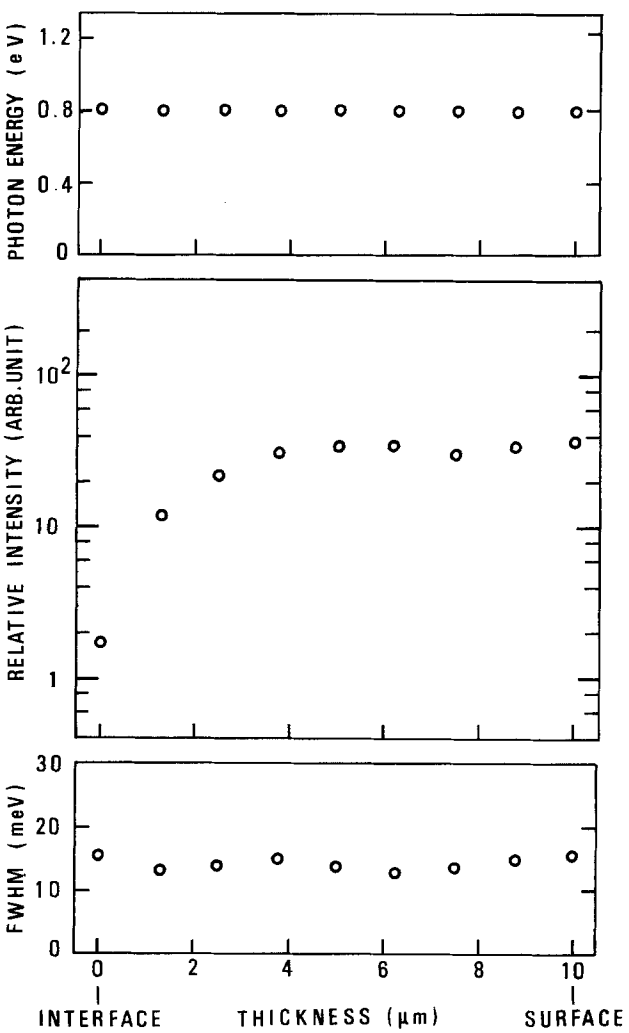


**Fig. 8. Variations of the photon energy at peak intensity, the intensity, and the FWHM along the angle-lapped cross section in sample 153, showing good composition homogeneity and uniform crystal quality.**

**Table III. Composition and electrical properties of mixed crystals and GaAs**

| $T_G$ (°C) | Sample No. | Composition $x$ | 300°K $\mu$* | 300°K n | 77°K $\mu$ | 77°K n |
|---|---|---|---|---|---|---|
| 550 | 183 | 0.44 | 5240 | $6.3 \times 10^{16}$ | 7,400 | $5.3 \times 10^{16}$ |
| 600 | 180 | 0.46 | 6590 | $3.2 \times 10^{16}$ | 11,700 | $2.7 \times 10^{16}$ |
| 650 | 177 | 0.47 | 8240 | $2.3 \times 10^{16}$ | 15,400 | $2.0 \times 10^{16}$ |
| 700 | 153 | 0.47 | 7600 | $5.0 \times 10^{15}$ | 20,200 | $4.3 \times 10^{15}$ |
| 750 | 173 | 0.47 | 8500 | $1.3 \times 10^{16}$ | 22,100 | $1.1 \times 10^{16}$ |
| 800 | 204 | 1.00 | 6920 | $2.0 \times 10^{14}$ | 46,400 | $1.9 \times 10^{14}$ |
| 800 | 211 | 1.00 | 6870 | $2.8 \times 10^{14}$ | 43,300 | $2.5 \times 10^{14}$ |

* $\mu$ (cm$^2$ V$^{-1}$ sec$^{-1}$), n (cm$^{-3}$).

Recently, Sankaran *et al.* (17) have reported mobility values of 10,030 cm$^2$ V$^{-1}$ sec$^{-1}$ at 300°K and 34,620 cm$^2$ V$^{-1}$ sec$^{-1}$ at 77°K in $In_{0.53}Ga_{0.47}As$ grown at 650°C by LPE on InP substrate, using the In, Ga, and As for the melt which was baked at 725°C for 22 hr. With the In, Ga, and InAs as melt constituents they have obtained 5540 cm$^2$ V$^{-1}$ sec$^{-1}$ at 300°K and 8430 cm$^2$ V$^{-1}$ sec$^{-1}$ at 77°K. Using almost the same purity In, Ga, and InAs, we have obtained mobility values of about 8000 cm$^2$ V$^{-1}$ sec$^{-1}$ at 300°K in the $In_{0.53}Ga_{0.47}As$ grown between 650° and 750°C by baking the In and Ga at 800°C for only 3 hr.

There has been a distinct difference in the value of the mobility between an epitaxial and a bulk $In_{1-x}Ga_xAs$ ($x \cong 0.5$), *i.e.*, the former has been lower and the latter similar to or higher than that of GaAs. Although Conrad *et al.* (7) suspected that the mixed crystal formation *per se* might be responsible in part for the low mobility and its temperature dependence, our results contradict this conclusion. The low mobility of the epitaxial layer grown previously can be considered to be due to a large internal strain and a large number of defects in the layer caused by the lattice mismatch with the substrate.

The electron concentration is calculated from the Hall coefficient using the relation

$$n = 1/eR_H$$

where $e$ is the electron charge and $R_H$ is the Hall coefficient. The Hall factor is assumed to be 1 for simplicity as is usually done. Figure 9 shows the electron concentration *vs.* inverse absolute temperature for three samples. The curve of a low concentration sample 173 shows two distinct regions suggesting two impurity levels at least; a shallow level for $T <$ 200°K and a deeper level for $T >$ 200°K. The distinction is not clear in the higher concentration samples. To find the donor and acceptor concentrations, a wider range of the temperature dependence of the electron concentration has to be measured and analyzed. However, it is evident from the temperature dependence of the mobilities that the impurity concentrations are not very high and the impurity scattering cannot be dominant at room temperature.

## Conclusions

Undoped $In_{1-x}Ga_xAs$ ($x \cong 0.5$) films were grown on the InP substrates by liquid phase epitaxy at temperatures between 550° and 750°C by the present growth process. Etch pit density, half-width of the

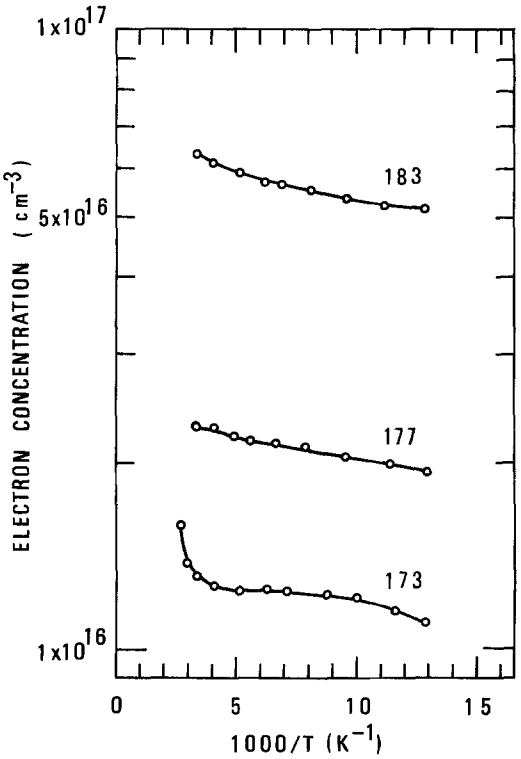


**Fig. 9. The electron concentration as a function of inverse absolute temperature. In sample 173, there are at least two impurity levels.**

PL spectra, and electron concentration decrease, while the electron mobilities at room temperature and at 77°K increase with increasing growth temperature. Composition and crystal quality are very uniform across the grown layer. The electron mobility is as high as 8500 $cm^2\ V^{-1}\ sec^{-1}$ at 300°K and increases on cooling from 300°K to 77°K in all samples. Although the crystal quality and the electrical properties seem to be better at high growth temperatures, the thermal decomposition of the InP substrate makes it difficult to obtain a uniform growth of the mixed crystal on the substrate. High quality crystals are grown at around 700°C.

## Acknowledgment

We are grateful to Dr. Shigeo Fujita for valuable discussions and experimental facilities and to Professor Tanaka's laboratory for x-ray diffractometer. It is a pleasure to acknowledge Mr. Yukio Naito for his assistance in the electrical measurements. This work was supported in part by the Grant-in-Aid for the specified subject "Crystal Growth" from Scientific Research of the Ministry of Education in Japan.

Manuscript submitted Aug. 16, 1976; revised manuscript received Aug. 22, 1977.

Any discussion of this paper will appear in a Discussion Section to be published in the December 1978 JOURNAL. All discussions for the December 1978 Discussion Section should be submitted by Aug. 1, 1978.

## REFERENCES

1. C. J. Nuese, M. Ettenberg, R. E. Enstrom, and H. Kressel, *Appl. Phys. Lett.*, **24**, 224 (1974).
2. R. E. Nahory, M. A. Pollack, and J. C. DeWinter, *ibid.*, **25**, 146 (1974).
3. C. J. Nuese and G. H. Olsen, *ibid.*, **26**, 528 (1975).
4. G. E. Stillman, C. M. Wolfe, A. G. Foyt, and W. T. Lindley, *ibid.*, **24**, 8 (1974).
5. L. G. Cohen, P. Kaiser, J. B. MacChesney, P. B. O'Conner, and H. M. Presby, *ibid.*, **26**, 472 (1975).
6. W. Fawcett, C. Hilsum, and H. D. Rees, *Electron. Lett.*, **5**, 313 (1969).
7. R. E. Conrad, P. L. Hoyt, and D. D. Martin, *This Journal*, **114**, 164 (1967).
8. B. J. Baliga and S. K. Ghandhi, *ibid.*, **122**, 683 (1975).
9. H. M. Manasevit and W. I. Simpson, *ibid.*, **120**, 135 (1973).
10. M. Glicksman, R. E. Enstrom, S. A. Mittleman, and J. R. Appert, *Phys. Rev. B*, **9**, 1621 (1974).
11. M. S. Abrahams, R. Braunstein, and F. D. Rosi, *J. Phys. Chem. Solids*, **10**, 204 (1959).
12. J. W. Wagner, *This Journal*, **117**, 1193 (1970).
13. T. V. Dzhakhutashvili, A. A. Mirtskhulava, L. G. Sakvarelidze, A. L. Shkol'nik, and M. S. Matinova, *Sov. Phys.-Semicond. (Engl. Trans.)*, **5**, 190 (1971).
14. R. E. Enstrom, D. Richman, M. S. Abrahams, J. A. Appert, D. G. Fisher, A. H. Sommer, and B. F. Williams, in "Gallium Arsenide and Related Compounds, 1970 Conference," Series 9, p. 30, Institute of Physics, London (1971).
15. H. Nagai and Y. Noguchi, *Appl. Phys. Lett.*, **26**, 108 (1975).
16. A. Sasaki, M. Mohri, T. Takagi, and T. Tanaka, Abstracts of the 4th International Conference on Crystal Growth, Tokyo, 1974, p. 237.
17. R. Sankaran, R. L. Moon, and G. A. Antypas, *J. Cryst. Growth*, **33**, 271 (1976).
18. Y. Takeda, A. Sasaki, Y. Imamura, and T. Takagi, *J. Appl. Phys.*, **47**, 5405 (1976).
19. T. Y. Wu and G. L. Pearson, *J. Phys. Chem. Solids*, **33**, 409 (1972).
20. J. C. Woolley and B. A. Smith, *Proc. Phys. Soc. (London)*, **72**, 214 (1958).
21. L. J. van der Pauw, *Philips Res. Rep.*, **13**, 1 (1958).
22. K. Pak, T. Nishinaga, and S. Uchiyama, *Jpn. J. Appl. Phys.*, **14**, 1613 (1975).
23. M. S. Abrahams and C. J. Buiocchi, *J. Appl. Phys.*, **36**, 2855 (1965).
24. J. L. Richards and A. J. Crocker, *J. Appl. Phys.*, **31**, 611 (1960).
25. G. B. Stringfellow, *ibid.*, **43**, 3455 (1972).
26. M. G. Astles, F. G. H. Smith, and E. W. Williams, *This Journal*, **120**, 1750 (1973).